cmgh
CELLULAR AND MOLECULAR GASTROENTEROLOGY AND HEPATOLOGY

ORIGINAL RESEARCH

Serotonin Activated Hepatic Stellate Cells Contribute to Sex Disparity in Hepatocellular Carcinoma

Qiqi Yang,[1,*] Chuan Yan,[1,2,*] Chunyue Yin,[3] and Zhiyuan Gong[1,2]

[1]Department of Biological Sciences, [2]Graduate School for Integrative Sciences and Engineering, National University of Singapore, Singapore; [3]Division of Gastroenterology, Hepatology and Nutrition, Cincinnati Children's Hospital Medical Center, Cincinnati, Ohio

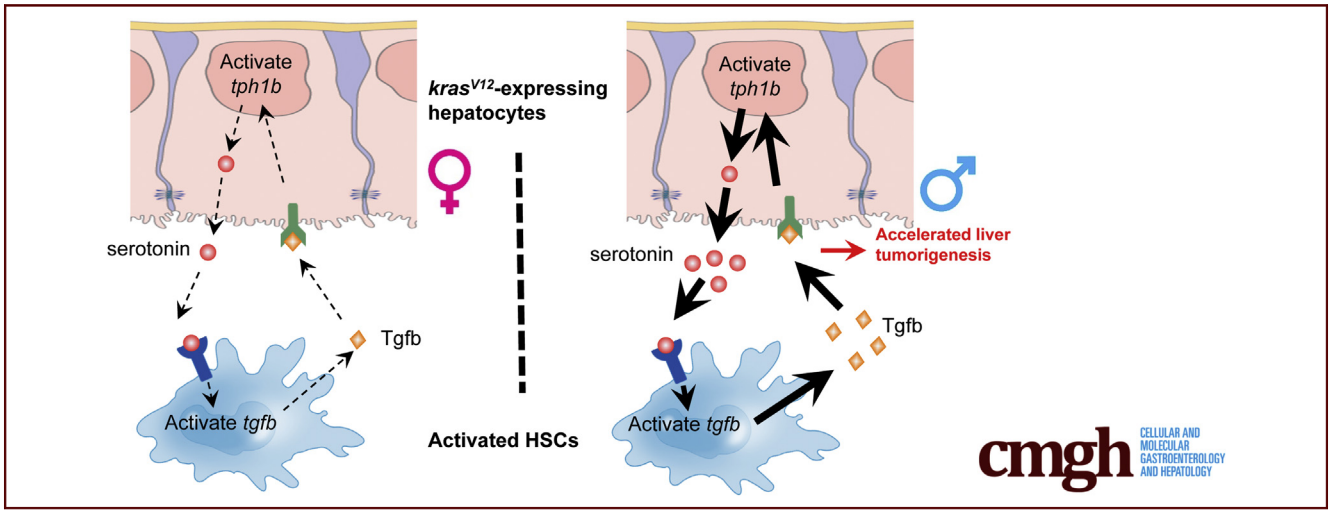

SUMMARY

A higher serotonin synthesis and accumulation in male zebrafish resulted in increased activation of hepatic stellate cells and transforming growth factor B1 expression and this has contributed to the accelerated progression of hepatocellular carcinoma in male zebrafish with activated *kras* oncogene expression.

BACKGROUND & AIMS: Hepatocellular carcinoma (HCC) occurs more frequently and aggressively in men than in women. Although sex hormones are believed to play a critical role in this disparity, the possible contribution of other factors largely is unknown. We aimed to investigate the role of serotonin on its contribution of sex discrepancy during HCC.

METHODS: By using an inducible zebrafish HCC model through hepatocyte-specific transgenic $kras^{V12}$ expression, differential rates of HCC in male and female fish were characterized by both pharmaceutical and genetic interventions. The findings were validated further in human liver disease samples.

RESULTS: Accelerated HCC progression was observed in $kras^{V12}$-expressing male zebrafish and male fish liver tumors were found to have higher hepatic stellate cell (HSC) density and activation. Serotonin, which is essential for HSC survival and activation, similarly were found to be synthesized and accumulated more robustly in males than in females. Serotonin-activated HSCs could promote HCC carcinogenesis and concurrently increase serotonin synthesis via transforming growth factor (Tgf)b1 expression, hence contributing to sex disparity in HCC. Analysis of liver disease patient samples showed similar male predominant serotonin accumulation and Tgfb1 expression.

CONCLUSIONS: In both zebrafish HCC models and human liver disease samples, a predominant serotonin synthesis and accumulation in males resulted in higher HSC density and activation as well as Tgfb1 expression, thus accelerating HCC carcinogenesis in males. *(Cell Mol Gastroenterol Hepatol 2017;3:484–499; http://dx.doi.org/10.1016/j.jcmgh.2017.01.002)*

Keywords: Liver Cancer; TGFB1; Kras; Zebrafish.

*Authors share co-first authorship.

Abbreviations used in this paper: α-SMA, α-smooth muscle actin; cDNA, complementary DNA; dox, doxycycline; EGFP, enhanced green fluorescence protein; Gfap, glial fibrillary acidic protein; HCC, hepatocellular carcinoma; HSC, hepatic stellate cell; Htr2b, 5-hydoxytryptamine receptor 2B; IF, immunofluorescence; IHC, immunohistochemistry; PCR, polymerase chain reaction; P-Tph1, phosphorylated tryptophan hydroxylase 1; TGF, transforming growth factor; Tph1, tryptophan hydroxylase 1; WT, wild type.

Most current article

2352-345X
http://dx.doi.org/10.1016/j.jcmgh.2017.01.002

See editorial on page 301.

Hepatocellular carcinoma (HCC) is notably more prevalent in men than in women, with a male-to-female ratio of 4.5:1.[1] The sex disparity appears to be mediated by a sex hormone–regulated mechanism. After menopause, women showed increased occurrence of HCC, which could be reduced with estrogen treatment.[2,3] In a carcinogen-induced mouse HCC model, administration of estrogen to male mice inhibited HCC development.[4] It is interesting to note that effects elicited by sex hormones are associated commonly with tumor microenvironment-mediated inflammatory response. For example, estrogen inhibits interleukin 6 expression in Kupffer cells (liver resident macrophages) and confers resistance to HCC in female mice.[5] Androgen signaling polarizes tumor-associated macrophages to a protumor gene expression profile during early hepatocarcinogenesis.[6] Interestingly, numerous HCC studies have shown a more robust and active HCC tumor microenvironment in males than in females. For example, infiltrating tumor-associated macrophage density has been found to be higher in males than in females in a mouse HCC model.[7] In human HCC patients, men have considerably higher numbers of intratumoral infiltrated CD66b+ neutrophils and CD8+ T cells; both are indicators of poor disease prognosis.[8]

Hepatic stellate cells (HSCs), the main fibrinogenic cell type in the liver, primarily are responsible for the production of extracellular matrix materials.[9–11] Recent studies have shown a tumor-promoting role of HSCs.[12] Tumor cell–secreted signals promote HSCs to transdifferentiate into highly proliferating myofibroblast-like cells, also known as activated HSCs.[13] Activated HSCs can induce phenotypic changes in cancer cells, primarily by secretion of protumor growth factors and cytokines such as hepatocyte growth factor and transforming growth factor (TGF)β1.[14] An increased HSC-specific gene expression signature in HCC patients indicates poor prognosis.[15] Notably, HSCs are found to be of higher density in male than in female HCC patients.[16] Because only activated HSCs rapidly proliferate, a higher HSC density in male HCC patients implies that a sex-dependent mechanism could contribute to activation of HSCs.[13]

Our laboratory previously generated several inducible HCC models by transgenic expression of an oncogene in hepatocytes in zebrafish.[17–21] The inducible nature of these zebrafish HCC models allows the oncogene to be activated at a given and controlled timing in both sexes, providing an excellent platform to study sex disparity in HCC initiation and progression. In this study, we attempted to investigate the mechanism of the sex disparity observed in HCC patients. In our *kras*^{V12}-expressing HCC zebrafish model, male fish showed accelerated carcinogenesis as compared with females.[17] Interestingly, we found an increased level of serotonin production in male *kras*^{V12}-expressing livers as compared with female counterparts and showed that serotonin was necessary for maintaining HSC survival and activation during HCC carcinogenesis. The activated HSCs in turn promoted HCC progression and at the same time increased serotonin synthesis in hepatocytes via Tgfb1, hence maintaining and promoting the sex disparity observed in *kras*^{V12}-expressing zebrafish. The findings in zebrafish were confirmed by our analyses of human liver disease patient samples, suggesting that serotonin is involved in the sex disparity of human HCC.

Materials and Methods

Zebrafish Husbandry

Zebrafish were maintained in compliance with Institutional Animal Care and Use Committee guidelines from the National University of Singapore. Five transgenic lines, *Tg(fabp10:rtTA2s-M2; TRE2:EGFP-kras*^{G12V}*)* (gz32Tg) in a tetracycline-controlled transcription activation (Tet-On) system for inducible hepatocyte-specific expression of oncogenic *kras*^{G12V},[17] *Tg(hand2:EGFP)* (pd24Tg) with EGFP-labeled HSCs under the hand2 promoter,[22] *Tg(tp1:EGFP)* (um14Tg) with EGFP-labeled cholangiocytes under a notch-responsive element,[23] *Tg(lyz:DsRed2)* (nz50Tg) with DsRed-labeled neutrophils under the lysozyme C (*lyz*) promoter,[24] *Tg(mpeg1:mCherry)* (gl22Tg), with mCherry-labeled macrophages under the *mpeg1* promoter,[25] and *Tg(fabp10:DsRed; ela3l:EGFP)* (gz15Tg) with DsRed-labeled hepatocytes under the *fabp10* promoter[26] were used in this study and referred to as *kras*+, *hand2*+, *lyz*+, *mpeg*+, and *fabp10*+, respectively, in the present report.

Chemical Treatment

All chemical/reagent treatments were conducted in 3-month-old adult fish for 7 days. The chemicals/reagents used included doxycycline (dox) (D9891; Sigma-Aldrich, St. Louis, MO), serotonin (14927; Sigma), PCPA (4-chloro-DL-phenylalanine) (C6506; Sigma), BW723C86 (B175; Sigma), SB204741 (S0693; Sigma), and SB431542 (1614; Tocris, Minneapolis, MN). Serotonin, PCPA, BW723C86, SB204741, SB431542, and dox were used for adult exposure at 10 μmol/L, 25 μmol/L, 15 μmol/L, 15 μmol/L, 2.5 μmol/L, and 30 μg/mL, respectively. The dosages were selected based on the highest all-survival concentrations in preliminary experiments.

Photography and Image Analysis

At each time point of chemical treatment experiments, more than 10 adult fish in each group were used for imaging analyses. These zebrafish were anesthetized in 0.08% tricaine (E10521; Sigma) and immobilized in 3% methylcellulose (M0521; Sigma) before imaging. Each zebrafish was photographed individually with an Olympus microscope (Olympus, Tokyo, Japan).

Isolation of Hepatocytes, Neutrophils, Macrophages, Cholangiocytes, and HSCs by Fluorescence-Activated Cell Sorting

Fabp10+, *lyz*+, *mpeg*+, *tp1*+, and *hand2*+ transgenic zebrafish in wild-type background were used for fluorescence-activated cell sorting isolation of hepatocytes, neutrophils, macrophages, cholangiocytes, and HSCs,

respectively, using a cell sorter (643245; BD Biosciences, Singapore). Ten adult livers were pooled and dissociated into single cells in the presence of 0.05% trypsin (T1426; Sigma) using a 40-μm mesh (352340; Fisher Scientific, Pittsburgh, PA) as previously described.[27] Hepatocytes (*fabp10*+), cholangiocytes (*tp1*+), and HSCs (*hand2*+) were isolated based on EGFP expression, neutrophils (*lyz*+) were isolated based on DsRed expression, and macrophages (*mpeg*+) were isolated based on mCherry expression.

RNA Extraction, Complementary DNA Amplification, and Reverse-Transcription Quantitative Polymerase Chain Reaction

Total RNA was extracted using the RNeasy mini kit (74104; Qiagen, Singapore). A total of 5 ng RNA was used as a template to synthesize and amplify complementary DNA (cDNA) using the QuantiTect Whole Transcriptome Kit (207043; Qiagen). Amplified cDNA was performed for real-time quantitative polymerase chain reaction (PCR) with LightCycler 480 SYBR Green I Master (04707516001; Roche, Singapore). Targeted cDNAs were amplified for 40 cycles (95°C, 20 s; 65°C, 15 s; and 72°C, 30 s). The sequences of PCR primers used were as follows: *β-actin*: CTCTGGGTCACCGCTTCTTT (forward) and CAGATGCTCACGAAACCCCT (reverse); *tph1b*: CTAAGAGCATACGGGGCTGG (forward) and GGACGCTGGATTGTCTTTGC (reverse); *htr2b*: CGCAGGATGTCCACCATAGG (forward) and TGCACCTTTCACAGAGCACA (reverse); and *tgfb1*: AGCAGAATTGCGTCTTCGGA (forward) and TCAAATGAGAGCCAGCGGTT (reverse).

Histologic and Cytologic Analyses

Ten adult livers were fixed in 4% paraformaldehyde in phosphate-buffered saline (P6748; Sigma), embedded in paraffin, and sectioned at 5-μm thickness using a microtome, followed by H&E, PicroSirus Red, Gomori's trichome, immunohistochemistry (IHC), or immunofluorescence (IF) stainings. H&E (H-3404; Vector Laboratories, Burlingame, CA, USA), Picrosirius Red (24901B; Polyscience, Inc, Warrington, PA), and Gomori's trichome (87021; Thermo Fisher Scientific, Singapore) stainings were conducted according to the manufacturers' protocols. For IHC and IF stainings, the primary antibodies were derived mostly from rabbits, including anti-proliferating cell nuclear antigen (PCNA) (FL-261; Santa Cruz Biotechnology, Dallas, TX), anti–caspase 3 (C92-065; BD Biosciences, Singapore), antiserotonin (C5545; Sigma), anti-TgfB1 (04-953; EMD Millipore, Billerica, MA), anti-PTph (SC135716; Santa Cruz), anti–α-smooth muscle actin (α-Sma) (ab15734; Abcam, Singapore), anti-PSmad2 (3101; Cell Signaling Technology, Danvers, MA) and anti–collagen I (ab23730; Abcam), except for anti-glial fibrillary acidic protein (Gfap) (154474; Abcam) from the mouse. Anti-rabbit or anti-mouse secondary antibodies were purchased from Thermo Fisher Scientific. At least 8 fish from each treatment group were examined and 1 high-power field was selected randomly from each fish liver and IF signals were counted manually for quantitative analyses.

Human Patient Samples

Paraffin-embedded human liver disease progression tissue microarray slides were purchased from Biomax, Inc (Derwood, MD) (LV8011a). Patients were classified into 4 groups: normal (n = 5), inflammation (n = 7), cirrhosis (n = 16), and HCC (n = 30). Histopathology of all patients was diagnosed by a pathologist based on the information provided from Biomax, Inc (https://www.biomax.us/tissue-arrays/Liver/LV8011a). Patient samples slides were subjected to H&E staining and IHC staining for serotonin and TGFβ1, respectively.

Statistical Analysis

Statistical significance between the 2 groups was evaluated by a 2-tailed unpaired Student *t* test using inStat version 5.0 for Windows (GraphPad, San Diego, CA). Statistical data are presented as means ± SDs.

Results

More Aggressive HCC Progression in Male $Kras^{V12}$-Expressing Livers

In human patients, men develop more aggressive HCC with larger tumors and a lower survival rate than women.[28–30] To examine if our $kras^{V12}$-expressing HCC zebrafish model recapitulated the sex disparity, male and female adult *kras*+ zebrafish were exposed to dox for 7 days. Initial gross morphologic examination of these *kras*+ zebrafish showed significantly enlarged livers in *kras*+ males than in *kras*+ females after 7 days of dox induction (Figure 1*A*). Histologically, $kras^{V12}$-expressing livers in males showed more advanced HCC phenotype than that in females. In males, $kras^{V12}$-expressing hepatocytes were densely situated with lost organization of the typical 2-cell hepatic plates; these are typical features of carcinoma. In contrast, female $kras^{V12}$-expressing livers were either hyperplastic or adenoma; these livers largely maintained the 2-cell plate but had a more prominent nucleoli and vacuolated cytoplasm (Figure 1*A*). As summarized in Figure 1*A*, 60% of female $kras^{V12}$-expressing livers showed adenoma histology and the remaining 40% had hepatic hyperplasia; in contrast, 100% of the male $kras^{V12}$-expressing livers showed carcinoma or adenoma histology.

To further investigate the mechanism behind this sex disparity, the cell proliferation, apoptosis, and extent of hepatic fibrosis were examined. As expected, $kras^{V12}$-expressing hepatocytes had higher rates of cell proliferation and apoptosis than their wild-type (WT) siblings (Figure 1*B* and *C*). When comparing the sexes, male $kras^{V12}$-expressing hepatocytes had a significantly higher numbers of proliferating but not apoptotic cells than female $kras^{V12}$-expressing hepatocytes. The extent of liver fibrosis could be a marker for early HCC.[31] By IF staining, male $kras^{V12}$-expressing livers showed a significantly higher expression of collagen I than WT siblings and also female $kras^{V12}$-expressing livers, reflecting its more advanced liver disease status (Figure 1*D*). Picrosirius Red and Gomori's trichrome staining, both of which stained for fibrotic tissues, showed consistent results with collagen I staining (Figure 1*E* and *F*).

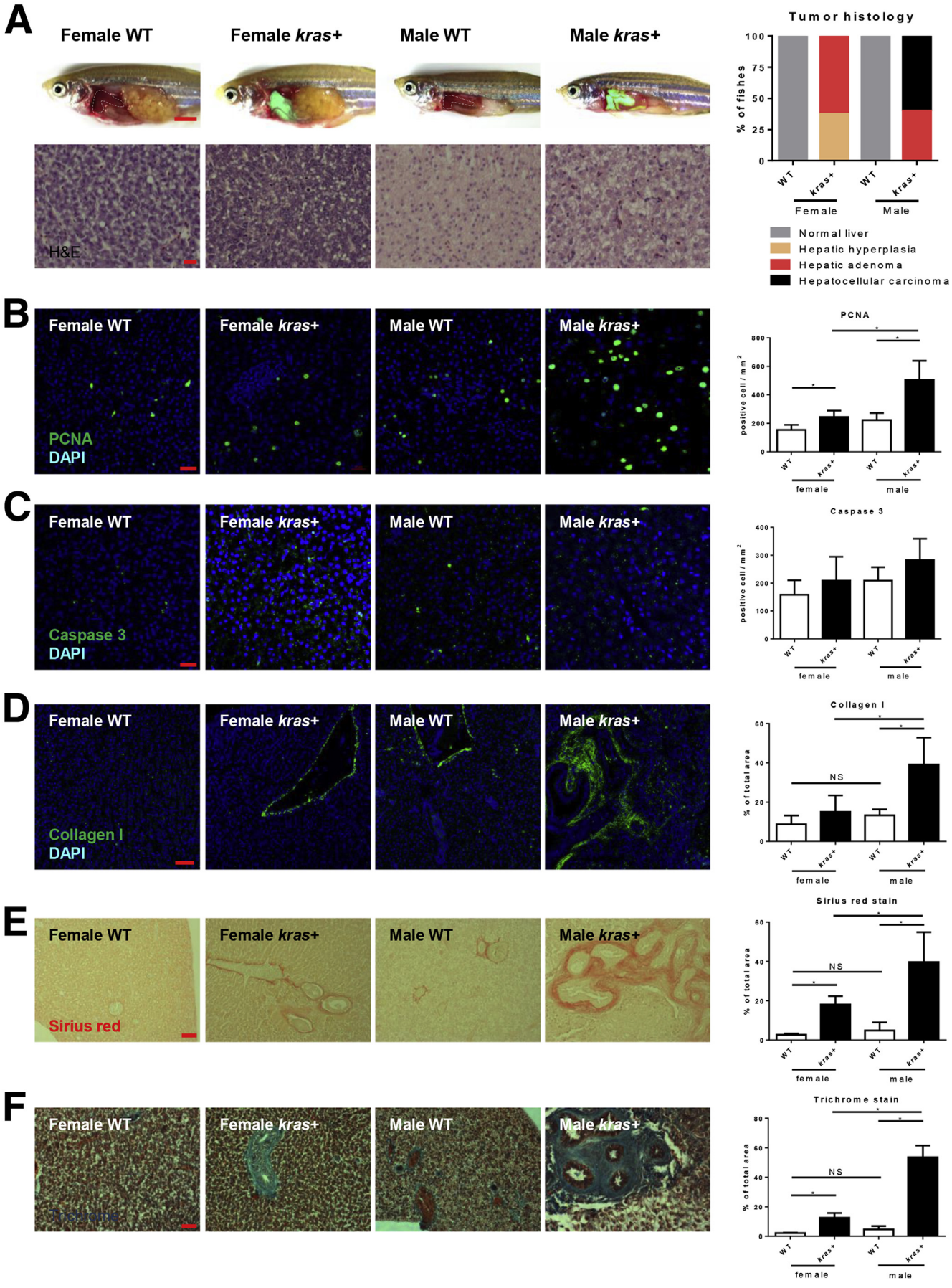
A
Female WT
Female kras+
Male WT
Male kras+
H&E
Tumor histology
% of fishes
100
75
50
25
0
WT
kras+
WT
kras+
Female
Male
Normal liver
Hepatic hyperplasia
Hepatic adenoma
Hepatocellular carcinoma
B
Female WT
Female kras+
Male WT
Male kras+
PCNA
DAPI
PCNA
positive cell / mm2
800
600
400
200
0
WT
kras+
WT
kras+
female
male
C
Female WT
Female kras+
Male WT
Male kras+
Caspase 3
DAPI
Caspase 3
positive cell / mm2
400
300
200
100
0
WT
kras+
WT
kras+
female
male
D
Female WT
Female kras+
Male WT
Male kras+
Collagen I
DAPI
Collagen I
% of total area
60
40
20
0
NS
WT
kras+
WT
kras+
female
male
E
Female WT
Female kras+
Male WT
Male kras+
Sirius red
Sirius red stain
% of total area
60
40
20
0
NS
WT
kras+
WT
kras+
female
male
F
Female WT
Female kras+
Male WT
Male kras+
Trichrome
Trichrome stain
% of total area
80
60
40
20
0
NS
WT
kras+
WT
kras+
female
male

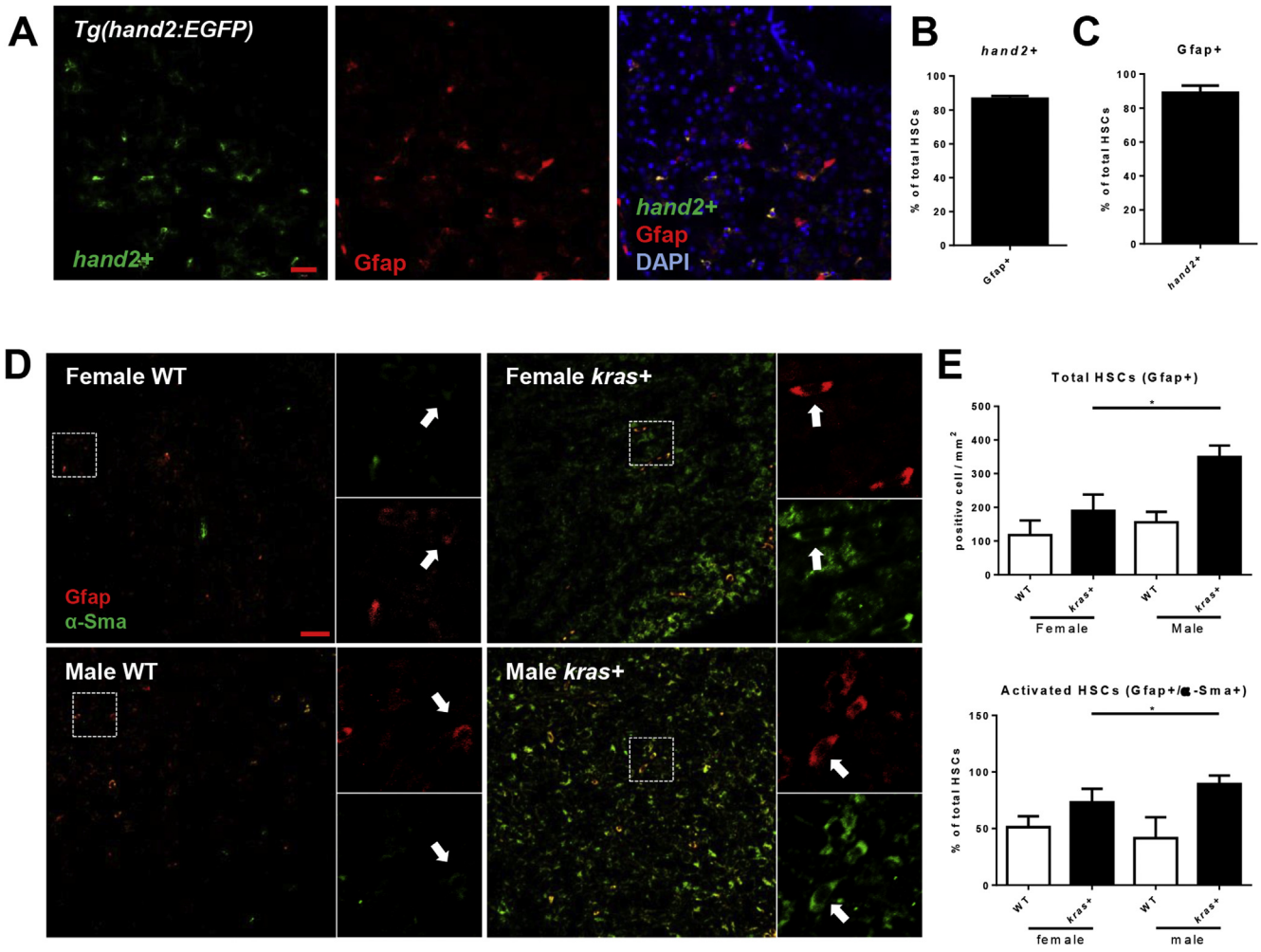

Figure 2. Sex disparate increase of HSCs and activated HSCs after *kras*^{V12} induction. (*A*) Overlap of hand2+ and Gfap expression. Gfap expression was examined in liver sections of *hand2*+ transgenic fish with 4′,6-diamidino-2-phenylindole (DAPI) staining for nuclei (blue) 8 days after fertilization. (*B*) Percentage of Gfap+ HSCs as marked by *hand2:gfp* expression in liver sections (n = 20). (*C*) Percentage of *hand2*+ HSCs as marked by Gfap+ expression in liver sections (n = 20). (*D*) IF co-staining of GFAP (red, general HSCs) and α-Sma (green, activated HSCs) in liver sections of adult zebrafish. Three-month-old *kras*+ and WT, male and female zebrafish were treated with 30 μg/mL dox for 7 days. Total HSCs, activated HSCs, and serotonin were examined. *White boxes* indicate enlarged regions shown on the right of each photograph. *Arrows* indicate Gfap+ cells. (*E*) Quantification of HSC density (Gfap+, *top*) and percentages of activated HSCs (Gfap+/α-Sma+, *bottom*) in liver sections (n > 8 in each group). *$P < .05$. *Scale bar*: 20 μm.

Figure 1. (***See previous page***). **Sex disparity in *kras*^{V12}-induced HCC progression.** Three-month-old adult zebrafish were treated with 30 μg/mL dox for 7 days and examined by various assays as described in the text. (*A*) Gross morphology and histology of *kras*+ and WT (control) male and female zebrafish after dox exposure. Male *kras*^{V12}-expressing liver (green for green fluorescent protein expression) were enlarged significantly as compared with female *kras*^{V12}-expressing liver and also with WT male and female livers (*dotted line enclosed*). *Bottom left*: H&E staining of the liver sections of dox-treated *kras*+ and WT (control) male and female zebrafish. *Right*: Quantification of tumor histology observed in the H&E-stained liver sections of dox-treated *kras*+ male and female zebrafish is shown (n = 10 each group). (*B–D*) IF staining of (*B*) PCNA, (*C*) caspase 3, and (*D*) collagen I in liver sections of dox-treated *kras*+ and WT male and female zebrafish. Quantifications of stained cells are shown on the *right* (n > 8 in each group). (*E*) Picrosirius Red staining of the liver sections of dox-treated *kras*+ and WT male and female zebrafish. Quantification of fibrotic liver tissue area in Picrosirius Red–stained liver sections is shown on the *right* (n > 10 in each group). (*F*) Gomori's trichrome staining of the liver sections of dox-treated *kras*+ and WT male and female zebrafish. Quantification of fibrotic liver tissue area in Gomori's trichrome–stained liver sections is shown on the *right* (n > 8 in each group). *$P < .05$. *Scale bars*: (*A*) 3 mm (*top row*), 20 μm (*bottom row*), (*E–F*) 500 μm, (*D*) 50 μm, and (*B* and *C*) 20 μm. DAPI, 4′,6-diamidino-2-phenylindole.

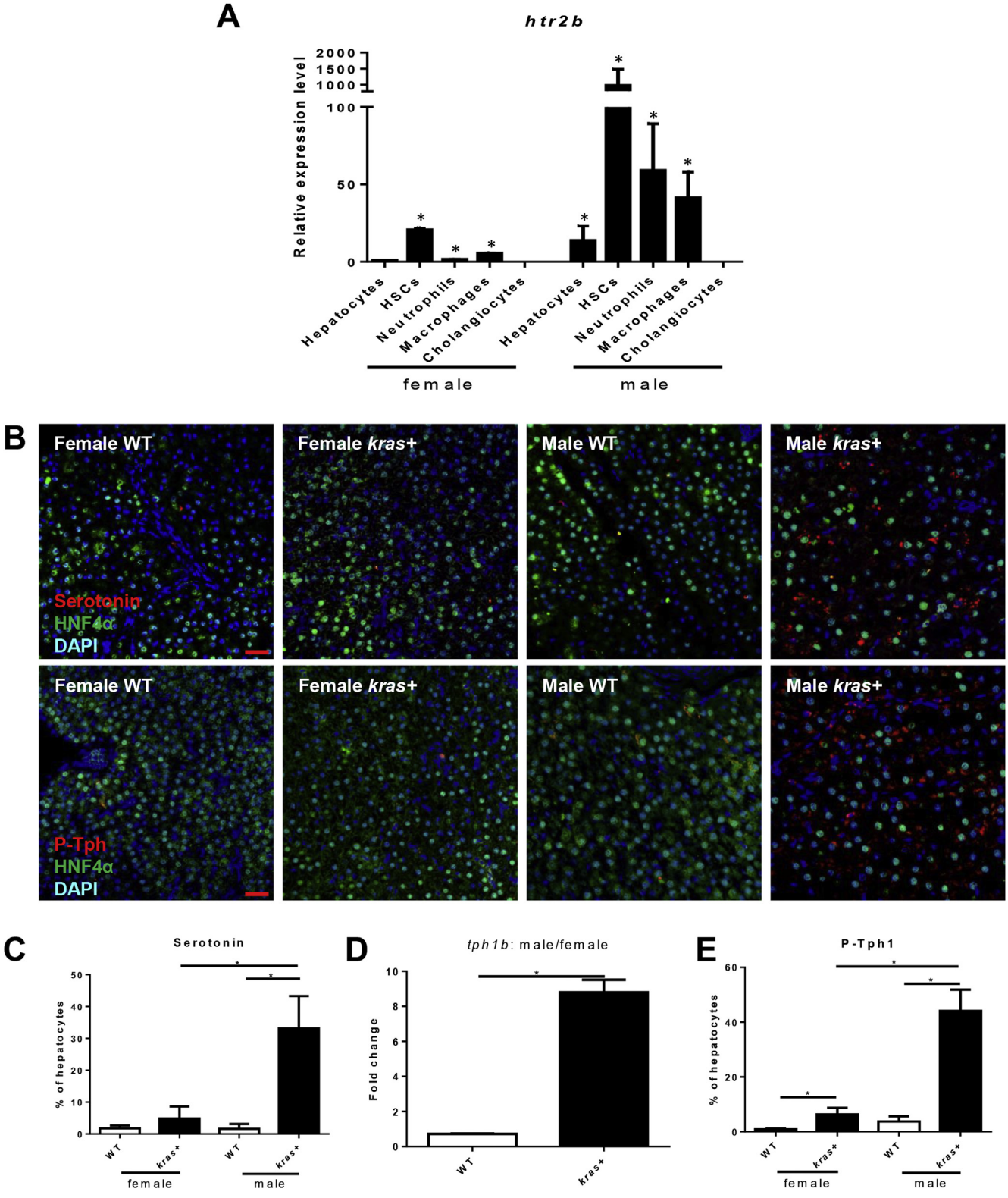
A
htr2b
Relative expression level
2000
1500
1000
100
50
0
Hepatocytes
HSCs
Neutrophils
Macrophages
Cholangiocytes
female
male
B
Female WT
Female kras+
Male WT
Male kras+
Serotonin
HNF4α
DAPI
P-Tph
C
Serotonin
% of hepatocytes
WT
kras+
female
male
D
tph1b: male/female
Fold change
E
P-Tph1

Accelerated Carcinogenesis in Male Kras^{V12}-Expressing Livers Correlated With Increased HSC Density and Serotonin Synthesis

In human HCC, male HCC patients have a higher HSC density than female patients and a high HSC density signals a poor prognosis.[15,16] Hence, HSC density and activation were investigated in our *kras*+ HCC zebrafish model. Gfap+ cells in the liver demarcate both activated and quiescent HSCs.[32] IF staining of Gfap on HSC reporter transgenic zebrafish, *hand2*+, showed nearly 90% *hand2*+ cells were positive for Gfap staining in the liver; similarly, 89% of Gfap+ cells were hand2+ cells (Figure 2*A*–*C*). Thus, there was high overlap between the 2 molecular markers for HSCs.[22] α-Sma is a marker for activated HSC[33]; hence, Gfap+/α-Sma+ cells in the liver were used to indicate activated HSCs (Figure 2*D*). With *kras*^{V12} expression, both total HSC density and the percentage of activated HSCs were significantly higher in male *kras*^{V12}-expressing livers than female (Figure 2*E*), indicating sex disparity in HSC activation in *kras*^{V12}-expressing livers.

Serotonin has been shown to play an activating role on HSCs via 5-hydoxytryptamine receptor 2B (Htr2b) in a mouse liver regeneration model.[34] To investigate if *htr2b* played a role in sex disparity in the *kras*+ HCC model in zebrafish, reverse-transcription quantitative PCR was performed in fluorescence-activated cell sorting–isolated hepatocytes, neutrophils, macrophages, HSCs and cholangiocytes. *Htr2b* was found to be expressed the most strongly in both male and female HSCs, with marginal expression in neutrophils and macrophages, but almost no expression was found in hepatocytes and cholangiocytes of both sexes (Figure 3*A*). Overall, the levels of *htr2b* expression was higher in males than in females in all cell types examined.

To account for the increased HSC density and activation, serotonin level was examined in male and female *kras*^{V12}-expressing livers. Interestingly, IF staining of serotonin indicated a more significantly increase in *kras*^{V12}-expressing hepatocytes in males than in females (Figure 3*B* and *C*). To investigate the sex difference in serotonin level, expression of tryptophan hydroxylase 1b (Tph1b), the rate-limiting enzyme for serotonin biosynthesis, was examined. Male *kras*^{V12}-expressing hepatocytes showed an 8-fold increase in *tph1b* messenger RNA expression (Figure 3*D*). Tph1 can undergo phosphorylation to enhance protein stability.[35] IF staining of phosphorylated Tph1 (P-Tph1) in liver sections showed a higher expression of the phosphorylated enzyme in male *kras*^{V12}-expressing hepatocytes than female *kras*^{V12}-expressing hepatocytes (Figure 3*B* and *E*), suggesting that the sex disparity in serotonin levels was owing to the higher expression and phosphorylation of Tph1b in males than in females.

Serotonin Promotes Kras^{V12}-Induced Carcinogenesis in Zebrafish via Activation of the Htr2b Receptor in HSCs

To examine if serotonin or Htr2b-receptor activation contributed significantly to the differential rates of HCC between sexes, serotonin and the Htr2b-receptor agonist BW723C86 were used to detect *kras*+ female zebrafish and the Tph1 inhibitor PCPA and the Htr2b-receptor antagonist SB204741 were used for *kras*+ male zebrafish for 7 days. Gross morphology of both serotonin- and BW723C86-treated *kras*+ females showed significantly enlarged livers as compared with WT control females. In contrast, *kras*+ male zebrafish showed a significant deterrence of liver enlargement with exposure to PCPA or SB204741 (Figure 4*A* and *B*). Histologically, exposure to serotonin or activation of the Htr2b receptor significantly accelerated the rate of carcinogenesis because an increased portion of female *kras*^{V12}-expressing livers showed a loss of 2-cell hepatic plates. However, decreased percentages of fish with HCC histology were observed in male *kras*^{V12}-expressing livers after exposure to PCPA or SB204741 (Figure 4*C*). As summarized in Figure 4*C*, 75% and 38% of female *kras*^{V12}-expressing livers showed HCC histology when exposed to serotonin and BW723C86, respectively. In contrast, 25% and 20% of male *kras*^{V12}-expressing livers showed milder histology when exposed to PCPA and SB204741, respectively.

Cytologic analysis of cell proliferation was consistent with morphologic and histologic changes. After 7 days of dox exposure, male *kras*^{V12}-expressing livers had a significantly higher level of proliferating cells than females. Exposure of serotonin or BW723C86 to *kras*+ females significantly increased the level of proliferating cells. Conversely, exposure of SB204741 and PCPA significantly reduced the number of proliferating cells (Figure 4*D*). In contrast, exposure to PCPA or SB204741 to *kras*+ males increased apoptotic liver cells significantly (Figure 4*E*). IF staining of collagen I, Picrosirius Red, or Gomori's trichrome staining consistently indicated an increased collagen deposition in the extracellular matrix when comparing male and female *kras*^{V12}-expressing livers (Figure 5). Exposure of

Figure 3. (***See previous page***). ***Htr2b* expression and serotonin production after *kras*^{V12} induction.** (*A*) Expression of *htr2b* in hepatocytes, HSCs, neutrophils, macrophages, and cholangiocytes. These cells were isolated by fluorescence-activated cell sorting based on DsRed, GFP, DsRed, mCherry, and GFP expression, respectively from *fabp10*+, *hand2*+, *lyz*+, *mpeg*+, and *tp1*+ transgenic zebrafish. Total RNA was extracted and *htr2b* expression was determined by reverse-transcription quantitative PCR. Relative expression levels are shown with the value from female hepatocytes set as 1. (*B*) IF co-staining of Hnf4a/Serotonin (*top*) and Hnf4a/P-Tph1 in liver sections. Three-month-old *kras*+ and WT, male and female zebrafish were treated with 30 μg/mL dox for 7 days. Serotonin and P-Tph level were examined. (*C*) Quantification of serotonin-positive hepatocytes in these zebrafish (n $>$ 8 in each group). (*D*) Reverse-transcription quantitative PCR determination of *tph1b* expression in hepatocytes isolated by fluorescence-activated cell sorting from dox-treated *kras*+ and *fabp10*+ (*kras*- control) male and female fish. Fold change is shown between males and females in WT and *kras*+ fish. (*E*) Quantification of percentage of P-Tph1–positive hepatocytes in these zebrafish (n $>$ 8 in each group). *$P < .05$. *Scale bar*: 20 μm. DAPI, 4′,6-diamidino-2-phenylindole.

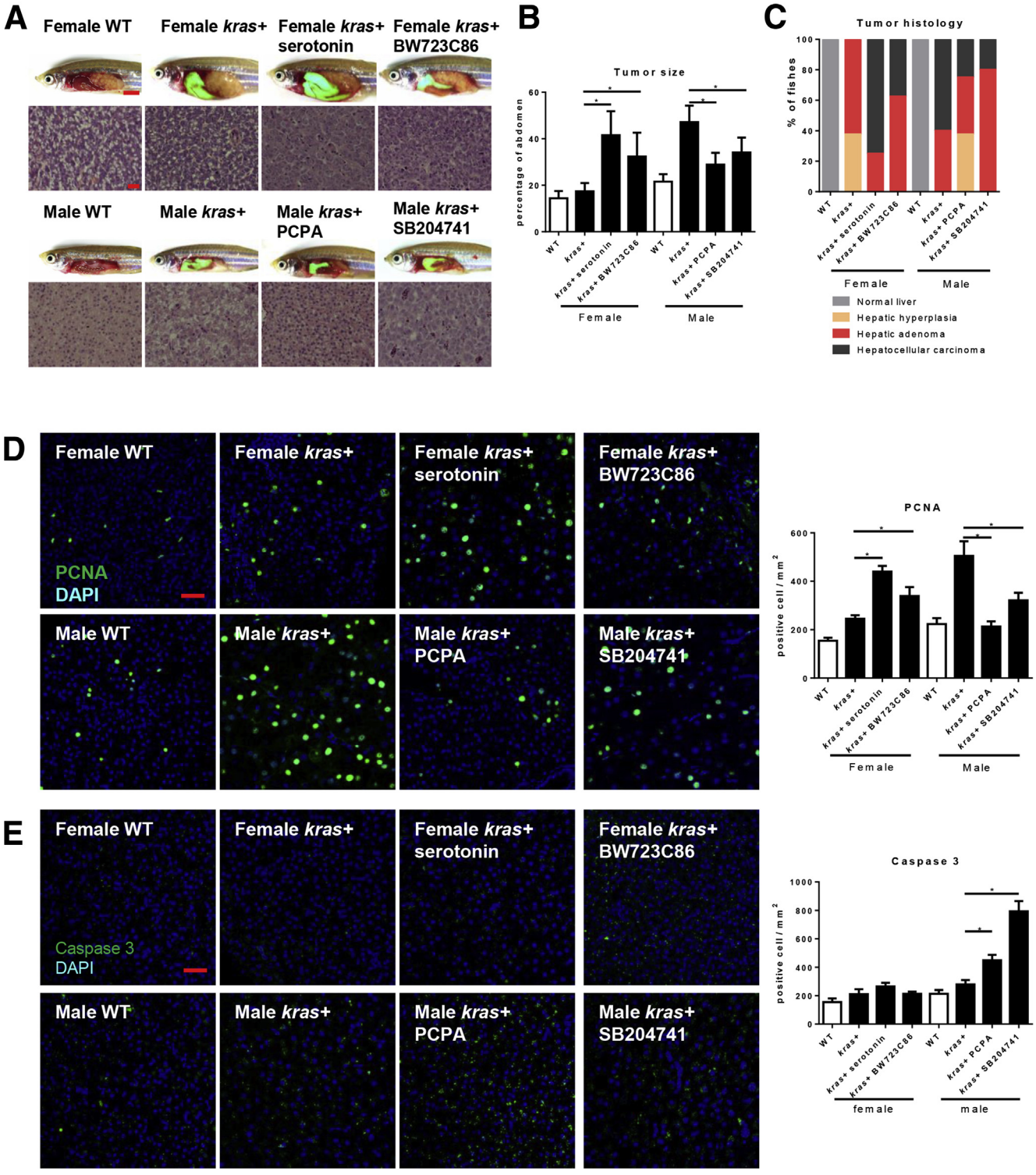

Figure 4. Effects of serotonin level and HSC activation on *kras*^{V12}-induced carcinogenesis. Three-month-old adult zebrafish were treated with dox with or without serotonin, BW23C86, PCPA, and SB204741 for 7 days. (*A*) Gross morphology and H&E staining of liver sections. (*B*) Quantification of tumor size as a percentage of total abdominal area. (*C*) Quantification of tumor histology observed in the H&E-stained liver sections of these zebrafish is shown on the *right* ($n > 8$ in each group). (*D* and *E*) IF staining and quantification of (*D*) PCNA+ and (*E*) caspase 3+ cells in liver sections of these zebrafish ($n > 8$). *$P < .05$. *Scale bars*: (*A*) 3 mm for gross observation images and 20 μm for histology images, and (*D* and *E*) 20 μm. DAPI, 4′,6-diamidino-2-phenylindole.

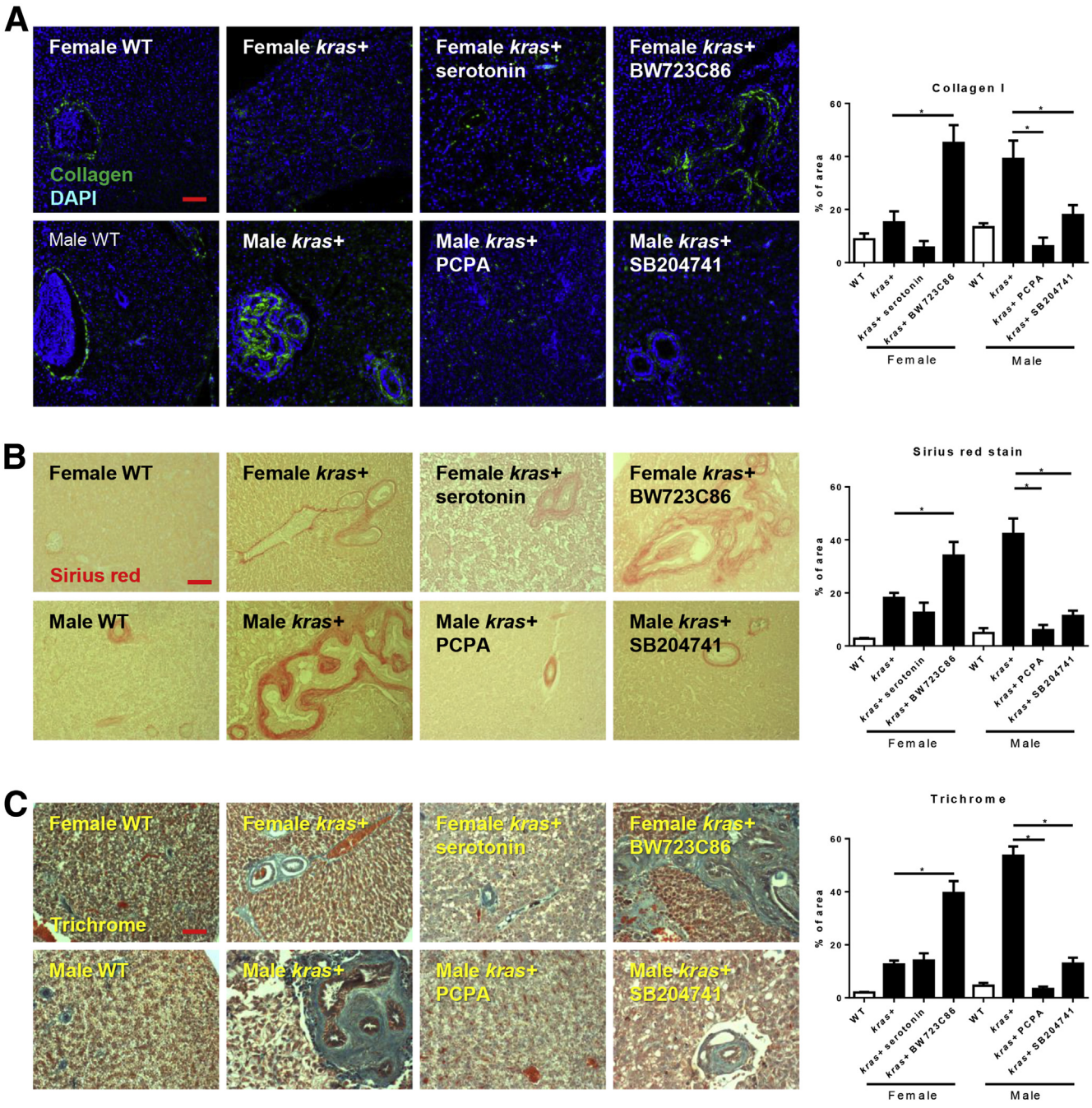

Figure 5. Effects of serotonin level and HSC activation on *kras*^{V12}-induced liver fibrosis. Three-month-old adult zebrafish were treated with dox with or without serotonin, BW23C86, PCPA, and SB204741 for 7 days. (*A*) IF staining of collagen I antibody and quantification of fibrotic liver tissue area in collagen I antibody–stained liver sections (n > 8 in each group). (*B*) Staining and quantification of fibrotic liver tissue area in Picrosirius Red–stained liver sections (n > 8 in each group). (*C*) Staining and quantification of fibrotic liver tissue area in Gomori's trichrome–stained liver sections (n > 8 in each group). *$P < .05$. *Scale bars*: (*A*) 50 μm, and (*B* and *C*) 500 μm. DAPI, 4′,6-diamidino-2-phenylindole.

kras+ female fish to BW723C86 increased collagen deposition as compared with *kras*+ female controls. In contrast, exposure to either SB204741 or PCPA decreased collagen deposition as compared with male *kras*+ control (Figure 5). Hence, either serotonin or the activation of the Htr2b receptor could accelerate carcinogenesis significantly in our *kras*^{V12}-expressing model.

Serotonin-Activated HSCs Promote Carcinogenesis and Serotonin Synthesis via Tgfb1

It has been reported previously that serotonin is capable of activating HSCs via the Htr2b receptor.[34] To investigate if serotonin was responsible for the sex disparity in HSC density through controlling the Htr2b downstream signaling, IF co-

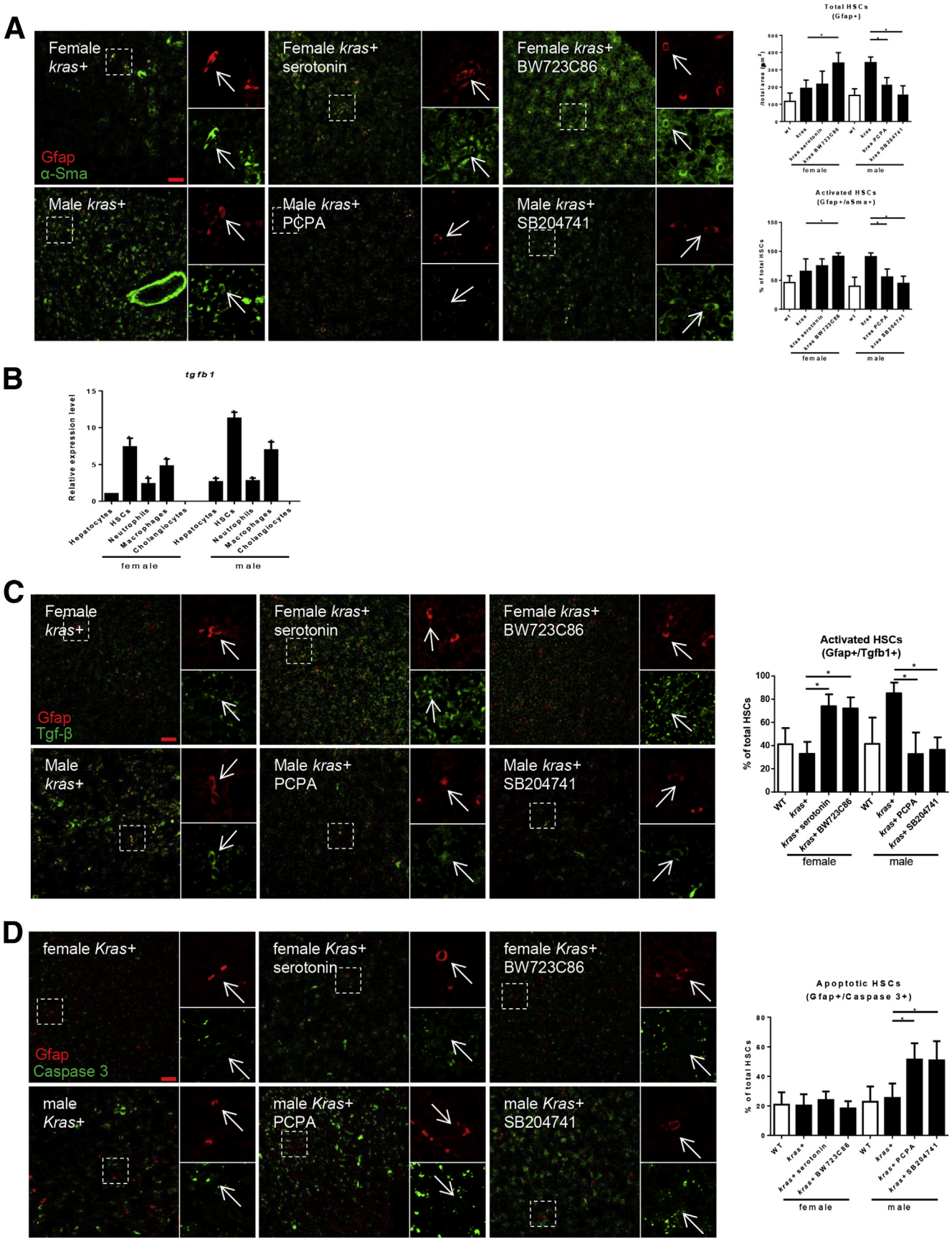
A
Female kras+
Gfap
α-Sma
Female kras+ serotonin
Female kras+ BW723C86
Male kras+
Male kras+ PCPA
Male kras+ SB204741
Total HSCs (Gfap+)
Activated HSCs (Gfap+/aSma+)
% of total HSCs
wt
kras
kras serotonin
kras BW723C86
kras PCPA
kras SB204741
female
male
B
tgfb1
Relative expression level
Hepatocytes
HSCs
Neutrophils
Macrophages
Cholangiocytes
female
male
C
Female kras+
Gfap
Tgf-β
Female kras+ serotonin
Female kras+ BW723C86
Male kras+
Male kras+ PCPA
Male kras+ SB204741
Activated HSCs (Gfap+/Tgfb1+)
% of total HSCs
WT
kras+
kras+ serotonin
kras+ BW723C86
kras+ PCPA
kras+ SB204741
female
male
D
female Kras+
Gfap
Caspase 3
female Kras+ serotonin
female Kras+ BW723C86
male Kras+
male Kras+ PCPA
male Kras+ SB204741
Apoptotic HSCs (Gfap+/Caspase 3+)
% of total HSCs
female
male

staining of Gfap and α-Sma was performed on both female and male *kras*^{V12}-expressing livers. As shown in Figure 6*A*, activation of Htr2b signaling by BW723C86 but not serotonin significantly increased both the total HSC density and percentage of activated HSCs whereas inhibition of serotonin synthesis by PCPA or inhibition of Htr2b signaling by SB204741 decreased both the density and percentage of activated HSCs, as compared with female or male *kras*^{V12}-expressing livers, respectively (Figure 6*A*). Thus, serotonin regulates HSCs through Htr2b, which could increase both the proliferation and activation of HSCs.

It has been reported that Htr2b activation is required for both HSC survival and *tgfb1a* expression.[34] To further elucidate the molecular outcome of Htr2b activation, expression of *tgfb1a* was examined in various cell types in the liver, including hepatocytes, HSCs, neutrophils, macrophages, and cholangiocytes. As shown in Figure 6*B*, HSCs had the highest level of *tgfb1a* expression in both male and female adult zebrafish (Figure 6*B*). Treatments with serotonin or BW723C86 significantly increased the percentage of Tgfb1-expressing HSCs in female *kras*^{V12}-expressing livers whereas treatments with PCPA or SB204741 significantly decreased HSCs of male *kras*^{V12}-expressing livers (Figure 6*C*). IF co-staining of Gfap with caspase-3 or Tgfb1 also was performed to show apoptotic HSCs (Gfap+/Cas3+). In contrast, the percentage of apoptotic HSCs remained unchanged in female *kras*^{V12}-expressing livers exposed to serotonin or BW723C86, but there was a significant increase in apoptotic HSCs in male *kras*^{V12}-expressing livers exposed to PCPA or SB204741 (Figure 6*D*). In contrast, therefore, serotonin activation of Htr2b signaling in HSCs is necessary for HSC survival as well as increased Tgfb1 expression.

Curiously, IF staining of serotonin indicated that BW723C8 activation of Htr2b in female *kras*^{V12}-expressing hepatocytes increased serotonin significantly, suggesting increased Tgfb1 or HSCs activation could promote serotonin synthesis (Figure 7*A*). To confirm the role of HSCs or Tgfb1 in serotonin synthesis, 3-month-old adult *kras*+ male zebrafish were exposed to either SB204741 or SB431542 (Tgfβ receptor 2 inhibitor) for 7 days. Inhibition of HSCs or Tgfβ signaling relaxed the HCC histology in male *kras*^{V12}-expressing livers (Figure 7*B*). Cytologic analysis of proliferating cells showed a significant decrease with both SB204741 and SB431541 exposure (Figure 7*C*). Tgfb1 is known to induce both cell senescence and apoptosis.[36,37] β-galactosidase staining for senescent cells showed no difference between 3-month-old adult *kras*+ female and *kras*+ male zebrafish after exposure to SB204741 or SB431542 (data not shown), whereas IF staining of caspase-3 showed significantly higher apoptotic cells with either SB204741 or SB431542 exposure to *kras*+ males (Figure 7*D*). Notably, both SB204741- and SB431542-treated zebrafish showed decreased Tgfb1 expression and corresponding down-regulation of phosphorylated Erk (P-Erk) and phosphorylated Smad2 (P-Smad2) signaling (Figure 7*E* and *F*), suggesting that inhibition of Htr2b-mediated HSC activation or inhibition of Tgfbr2 decreased both Tgfb1 expression and its downstream signaling. Interestingly, inhibition of both HSC activation and Tgfβ1 signaling showed an inhibition of Tph1 phosphorylation and hence the serotonin production (Figure 7*G* and *H*), suggesting a potential role of HSC and their secreted Tgfb1 in regulating Tph1 activity.

Sex Differences in Serotonin and TGFB1 Level in Human Liver Disease Patients

In human liver diseases, serum serotonin levels have been shown to increase significantly in patients with cirrhosis and HCC.[38] To observe if the sex disparate serotonin levels observed in our *kras*^{V12} HCC zebrafish model would be reflected in human patients, a panel of liver disease samples, including normal, liver inflammation, cirrhosis, and HCC, were analyzed for levels of serotonin and TGFB1. Each sample then was stained for H&E, serotonin, and TGFB1, respectively (Figure 8*A*–*C*). Notably, serotonin levels in inflammation and cirrhosis samples were significantly higher in males than in females (Figure 8*D*). This sex disparity was less evident in HCC samples but still was very significant. Similarly, male-biased TGFB1 expression also was evident in inflammation, cirrhosis, and HCC samples (Figure 8*E*). Serotonin and TGFB1 protein showed a positive and significant correlation in both inflammation and cirrhosis patients, suggesting the molecular mechanism of serotonin-induced TGFB1 expression potentially translated in this cohort of patients. However, the correlation between the 2 molecules was abrogated in HCC patients, suggesting other confounding factors might contribute to TGFB1 expression in HCC patients (Figure 8*F-H*).

Discussion

Higher Expression of Serotonin in Males Contributed to Sex Disparity via Htr2b Activation of HSCs

In our investigation of human liver disease samples, serotonin levels were increased significantly in inflammation and cirrhosis, and marginally in HCC samples as

Figure 6. (***See previous page***). **Manipulation of serotonin level and HSC density affects HSC activation and apoptosis.** (*A*) IF staining and quantification of HSC density (Gfap+) in liver sections (n > 8 in each group). Three-month-old adult zebrafish were treated with dox with or without serotonin, BW23C86, PCPA, and SB204741 for 7 days. Percentages of activated HSCs (Gfap+/α-Sma+) in the liver sections (n > 8 in each group). (*B*) Expression of *tgfb1* in hepatocytes, HSCs, neutrophils, macrophages, and cholangiocytes. These cells were isolated by fluorescence-activated cell sorting based on DsRed, GFP, DsRed, mCherry, and GFP expression, respectively, from *fabp10*+, *hand2*+, *lyz*+, *mpeg*+, and *tp1*+ transgenic zebrafish. Total RNAs were extracted and *htr2b* expression was determined by reverse-transcription quantitative PCR. Relative expression levels are with the values with female hepatocytes set as 1. (*C* and *D*) IF staining and quantification of percentages of (*C*) TgfB1+ HSCs (Gfap+/Tgfb1+) and (*D*) apoptotic HSCs in the liver sections as described in panel *A*. n > 8 in each group. *$P < .05$. *Scale bar*: 20 μm.

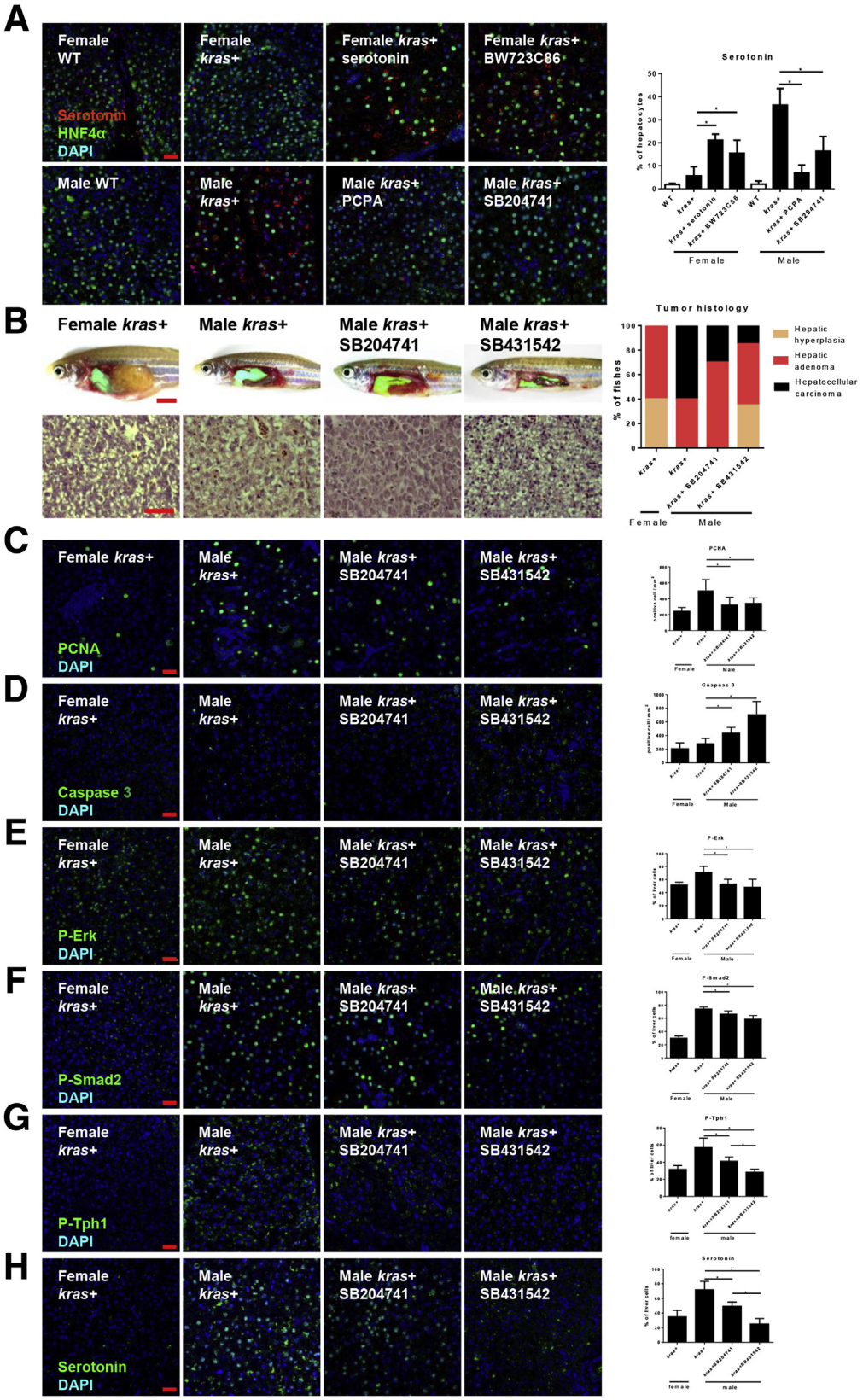

Figure 7. Tgfb1 promotes serotonin synthesis and *kras*^{V12}-induced carcinogenesis. Three-month-old adult zebrafish were treated for 7 days with 30 μg/mL dox with or without 2 μmol/L serotonin, BW23C86, PCPA, and SB204741. (*A*) IF staining of serotonin in liver section of these zebrafish. These slides also were co-stained for hepatocytes (HNF4a) and nuclei (4′,6-diamidino-2-phenylindole [DAPI]). *Right*: Quantification of serotonin-positive liver cells as percentages of hepatocytes (n = 10). Three-month-old Male *kras*^{V12}-expressing zebrafish were treated with dox with or without SB204741 and SB431542, respectively. (*B*) Gross morphology and H&E staining of liver sections of these zebrafish. Quantification of tumor histology observed in the H&E-stained liver sections of these zebrafish (n > 8 in each group). (*C–H*) IF staining and quantification of (*C*) PCNA+, (*D*) caspase 3+, (*E*) P-Erk+, (*F*) P-Smad2, (*G*) P-Tph+, and (*H*) serotonin+ cells in liver sections (n > 8 in each group). *P < .05. *Scale bars*: (*B*) 3 mm (*top row*) and 50 μm (*bottom row*), and (*A, C–H*) 20 μm.

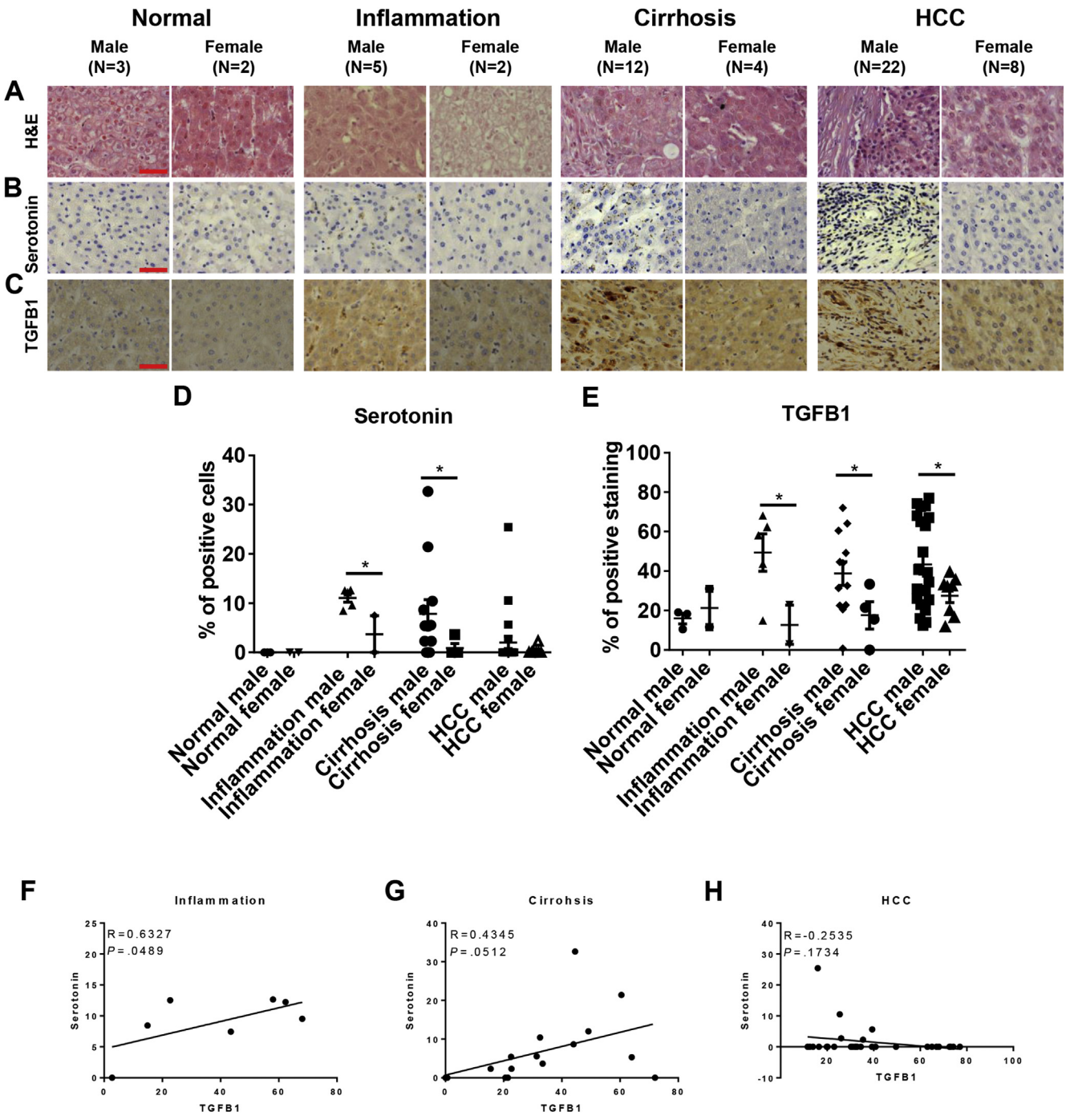

Figure 8. Sex difference in serotonin and TGFB1 levels in human liver disease samples. A panel of liver disease samples from human patients was examined for histology by H&E staining and for serotonin and TGFB1 levels by antibody staining. These samples were categorized into normal, inflammation, cirrhosis, and HCC for both males and females. (*A*) H&E staining of human liver disease samples. (*B* and *C*) IHC staining of antibody against (*B*) serotonin and (*C*) TGFB1. (*D* and *E*) Quantification of the percentages of (*D*) serotonin or (*E*) TGFB1-positive liver cells in inflammation, cirrhosis, and HCC patients. (*F–H*) Quantification of correlation between serotonin with TGFB1 in (*F*) inflammation, (*G*) cirrhosis, and (*H*) HCC patients. *$P < .05$. *Scale bar*: 20 μm.

compared with normal liver control samples. This is consistent with a previous observation that serotonin was a more sensitive serum marker for cirrhosis and HCC than α-fetoprotein.[32] The level of serotonin in HCC was significantly lower than in inflammation and cirrhosis samples, suggesting that the contribution of serotonin to liver diseases is possibly more important in early phases of the progression to HCC. Notably, in the cohort of human patients we analyzed, an apparent sex-dependent accumulation was observed in both inflammation and cirrhosis

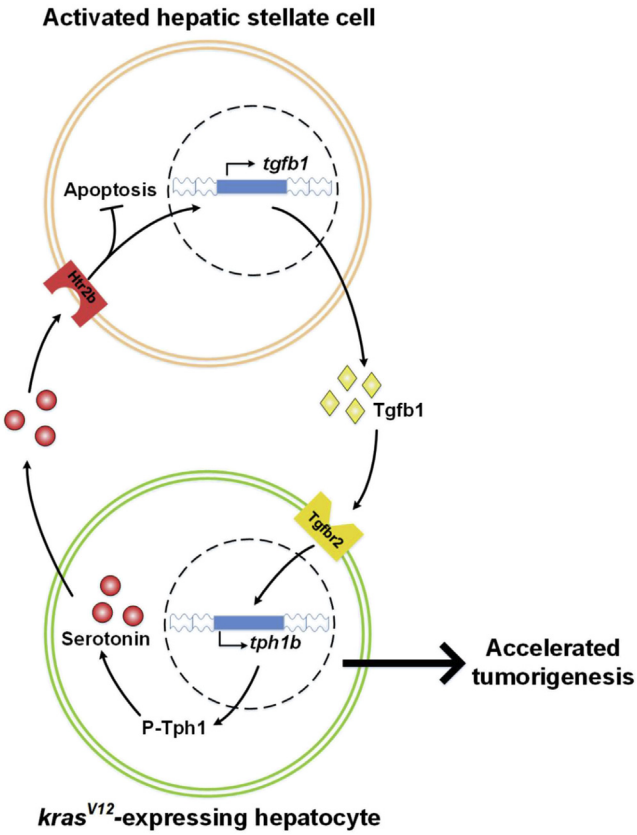

Figure 9. Schematic summary of serotonin-activated HSCs and Tgfb signal in accelerating liver tumorigenesis in *kras*+-expressing male transgenic fish.

samples because serotonin was generally not detected in female patients of both stages. This is in line with the prevailing knowledge that men have a significantly higher rate of serotonin synthesis than women.[39] Our zebrafish studies recapitulated the sex disparity of serotonin accumulation, which likely can be attributed to the difference in the expression and phosphorylation of rate-limiting enzyme Tph1a. A previously conducted study suggested androgen to be responsible for the activation of Tph1 in macaques, thus providing a link to the sex difference in serotonin.[40] The sex differential production of serotonin and HSC density and activation also similarly were observed in other oncogene-induced (*xmrk* and *Myc*) zebrafish HCC models generated in our laboratory[18,19]; thus, the involvement of serotonin and HSCs in the sex disparity of HCC is not oncogene-specific (our unpublished observations).

Serotonin can act on a variety of serotonin receptors. We showed that Htr2b was highly expressed in HSCs, consistent with a previously reported mouse study.[34] The sex disparity in serotonin synthesis resulted in a higher rate of Htr2b-mediated activation of HSCs in males than in females, and led to both a higher density of total HSCs and a higher percentage of activated HSCs, in line with a human HCC patient study in which male patients had a higher density of HSCs than female patients.[16] In this study, increased Htr2b activation in HSCs resulted in overexpression of Tgfb1. Both inactivation of HSCs and depletion of TgfB1 signaling significantly relaxed the rate of carcinogenesis in male $kras^{V12}$-expressing livers, consistent with the current notion that TGFB1 acts as a protumor cytokine in human HCC.[41]

HSCs Maintain Sex Disparity in HCC via a Serotonin/Tgfβ1 Loop

In our zebrafish study, serotonin level was found to be dependent on Htr2b activation. A role of TGFB1 in the regulation of TPH1 expression and phosphorylation via ERK and SMAD pathways has been shown in human cells.[42,43] Depletion of HSCs via Htr2b antagonist and inhibition of Tgfβ signaling in $kras^{V12}$-expressing livers of male zebrafish inhibited P-Tph1 and serotonin expression, suggesting that the role of activated HSCs on serotonin synthesis is mediated by Tgfβ signaling. Hence, the robust activation of HSCs via Htr2b in male $kras^{V12}$-expressing livers would establish a positive feedback loop, ensuring constant and high levels of serotonin synthesis, thus accelerating carcinogenesis via the multifunctional cytokine, Tgfb1. Although this molecular mechanism similarly would exist in female $kras^{V12}$-expressing livers, the lower initial P-Tph level would result in the initiation of a less-robust feedback loop. This is at least in part consistent with our analyses on human liver disease samples. TGFB1 showed a similar sex-biased expression in inflammation, cirrhosis, and HCC patients. However, significant correlation between serotonin and TGFB1 was observed only in inflammation and cirrhosis samples but not in HCC patients, possibly because of many other factors affecting TGFB1 expression during carcinogenesis.

In summary, as shown in Figure 9, data from both zebrafish models and human liver disease samples showed the differential accumulation of serotonin during liver disease progression between sexes, which could be attributed to the disparity of P-Tph level in the 2 sexes of *kras*+ zebrafish. We further showed the novel role of serotonin in initiating and promoting a sex-disparate tumor microenvironment via Htr2b activation of HSCs. Htr2b-activated HSCs expressed Tgfb1, which not only promoted HCC progression but also increased serotonin synthesis. Hence, HSCs not only promote liver tumor progression but also play a vital role in maintaining the sex disparity observed in HCC patients.

References

1. Lee CM, Lu SN, Changchien CS, et al. Age, gender, and local geographic variations of viral etiology of hepatocellular carcinoma in a hyperendemic area for hepatitis B virus infection. Cancer 1999;86:1143–1150.
2. Mucci LA, Kuper HE, Tamimi R, et al. Age at menarche and age at menopause in relation to hepatocellular carcinoma in women. BJOG 2001;108:291–294.
3. Yu MW, Chang HC, Chang SC, et al. Role of reproductive factors in hepatocellular carcinoma: impact on hepatitis B- and C-related risk. Hepatology 2003;38:1393–1400.
4. Nakatani T, Roy G, Fujimoto N, et al. Sex hormone dependency of diethylnitrosamine-induced liver tumors in

mice and chemoprevention by leuprorelin. Jpn J Cancer Res 2001;92:249–256.
5. Naugler WE, Sakurai T, Kim S, et al. Gender disparity in liver cancer due to sex differences in MyD88-dependent IL-6 production. Science 2007;317:121–124.
6. Wolf MJ, Adili A, Piotrowitz K, et al. Metabolic activation of intrahepatic CD8+ T cells and NKT cells causes nonalcoholic steatohepatitis and liver cancer via cross-talk with hepatocytes. Cancer Cell 2014;26:549–564.
7. Yang W, Lu Y, Xu Y, et al. Estrogen represses hepatocellular carcinoma (HCC) growth via inhibiting alternative activation of tumor-associated macrophages (TAMs). J Biol Chem 2012;287:40140–40149.
8. Li YW, Qiu SJ, Fan J, et al. Intratumoral neutrophils: a poor prognostic factor for hepatocellular carcinoma following resection. J Hepatol 2011;54:497–505.
9. Krizhanovsky V, Yon M, Dickins RA, et al. Senescence of activated stellate cells limits liver fibrosis. Cell 2008; 134:657–667.
10. Bocca C, Novo E, Miglietta A, et al. Angiogenesis and fibrogenesis in chronic liver diseases. Cell Mol Gastroenterol Hepatol 2015;1:477–488.
11. Roth KJ, Copple BL. Role of hypoxia-inducible factors in the development of liver fibrosis. Cell Mol Gastroenterol Hepatol 2015;1:589–597.
12. Hirsova P, Gores GJ. Death receptor-mediated cell death and proinflammatory signaling in nonalcoholic steatohepatitis. Cell Mol Gastroenterol Hepatol 2015; 1:17–27.
13. Amann T, Bataille F, Spruss T, et al. Activated hepatic stellate cells promote tumorigenicity of hepatocellular carcinoma. Cancer Sci 2009;100:646–653.
14. Kang N, Gores GJ, Shah VH. Hepatic stellate cells: partners in crime for liver metastases? Hepatology 2011; 54:707–713.
15. Ji J, Eggert T, Budhu A, et al. Hepatic stellate cell and monocyte interaction contributes to poor prognosis in hepatocellular carcinoma. Hepatology 2015;62:481–495.
16. Dai CX, Gao Q, Q SJ, et al. Hypoxia-inducible factor-1 alpha, in association with inflammation, angiogenesis and MYC, is a critical prognostic factor in patients with HCC after surgery. BMC Cancer 2009;9:418.
17. Chew TW, Liu XJ, Liu L, et al. Crosstalk of Ras and Rho: activation of RhoA abates Kras-induced liver tumorigenesis in transgenic zebrafish models. Oncogene 2014; 33:2717–2727.
18. Li Z, Huang X, Zhan H, et al. Inducible and repressable oncogene-addicted hepatocellular carcinoma in Tet-on xmrk transgenic zebrafish. J Hepatol 2012;56:419–425.
19. Li Z, Zheng W, Wang Z, et al. A transgenic zebrafish liver tumor model with inducible Myc expression reveals conserved Myc signatures with mammalian liver tumors. Dis Model Mech 2013;6:414–423.
20. Nguyen AT, Emelyanov A, Koh CH, et al. An inducible kras(V12) transgenic zebrafish model for liver tumorigenesis and chemical drug screening. Dis Model Mech 2012;5:63–72.
21. Sun L, Nguyen AT, Spitsbergen JM, et al. Myc-induced liver tumors in transgenic zebrafish can regress in tp53 null mutation. PLoS One 2015;10:e0117249.
22. Yin C, Evason KJ, Maher JJ, et al. The basic helix-loop-helix transcription factor, heart and neural crest derivatives expressed transcript 2, marks hepatic stellate cells in zebrafish: analysis of stellate cell entry into the developing liver. Hepatology 2012;56:1958–1970.
23. Parsons MJ, Pisharath H, Yusuff S, et al. Notch-responsive cells initiate the secondary transition in larval zebrafish pancreas. Mech Dev 2009;126:898–912.
24. Hall C, Flores MV, Storm T, et al. The zebrafish lysozyme C promoter drives myeloid-specific expression in transgenic fish. BMC Dev Biol 2007;7:42.
25. Ellett F, Pase L, Hayman JW, et al. mpeg1 promoter transgenes direct macrophage-lineage expression in zebrafish. Blood 2011;117:e49–e56.
26. Korzh S, Pan X, Garcia-Lecea M, et al. Requirement of vasculogenesis and blood circulation in late stages of liver growth in zebrafish. BMC Dev Biol 2008;8:84.
27. Manoli M, Driever W. Fluorescence-activated cell sorting (FACS) of fluorescently tagged cells from zebrafish larvae for RNA isolation. Cold Spring Harb Protoc 2012; 2012:8.
28. Dohmen K, Shigematsu H, Irie K, et al. Longer survival in female than male with hepatocellular carcinoma. J Gastroenterol Hepatol 2003;18:267–272.
29. Farinati F, Sergio A, Giacomin A, et al. Is female sex a significant favorable prognostic factor in hepatocellular carcinoma? Eur J Gastroenterol Hepatol 2009; 21:1212–1218.
30. Hefaiedh R, Ennaifer R, Romdhane H, et al. Gender difference in patients with hepatocellular carcinoma. Tunis Med 2013;91:505–508.
31. Huang M, Chang A, Choi M, et al. Antagonistic interaction between Wnt and Notch activity modulates the regenerative capacity of a zebrafish fibrotic liver model. Hepatology 2014;60:1753–1766.
32. Morini S, Carotti S, Carpino G, et al. GFAP expression in the liver as an early marker of stellate cells activation. Ital J Anat Embryol 2005;110:193–207.
33. Carpino G, Morini A, Ginanni Corradini S, et al. Alpha-SMA expression in hepatic stellate cells and quantitative analysis of hepatic fibrosis in cirrhosis and in recurrent chronic hepatitis after liver transplantation. Dig Liver Dis 2005;37:349–356.
34. Ebrahimkhani MR, Oakley F, Murphy LB, et al. Stimulating healthy tissue regeneration by targeting the 5-HT(2)B receptor in chronic liver disease. Nat Med 2011; 17:1668–1673.
35. Huang Z, Liu T, Chattoraj A, et al. Posttranslational regulation of TPH1 is responsible for the nightly surge of 5-HT output in the rat pineal gland. J Pineal Res 2008; 45:506–514.
36. Senturk S, Mumcuoglu M, Gursoy-Yuzugullu O, et al. Transforming growth factor-beta induces senescence in hepatocellular carcinoma cells and inhibits tumor growth. Hepatology 2010;52:966–974.
37. Jang CW, Chen CH, Chen CC, et al. TGF-beta induces apoptosis through Smad-mediated expression of DAP-kinase. Nat Cell Biol 2002;4:51–58.
38. Abdel-Razik A, Elhelaly R, Elzehery R, et al. Could serotonin be a potential marker for hepatocellular

carcinoma? A prospective single-center observational study. Eur J Gastroenterol Hepatol 2016; 28:599–605.
39. Nishizawa S, Benkelfat C, Young SN, et al. Differences between males and females in rates of serotonin synthesis in human brain. Proc Natl Acad Sci U S A 1997; 94:5308–5313.
40. Bethea CL, Reddy AP, Robertson N, et al. Effects of aromatase inhibition and androgen activity on serotonin and behavior in male macaques. Behav Neurosci 2013; 127:400–414.
41. Giannelli G, Villa E, Lahn M. Transforming growth factor-beta as a therapeutic target in hepatocellular carcinoma. Cancer Res 2014;74:1890–1894.
42. Imbe H, Senba E, Kimura A, et al. Activation of mitogen-activated protein kinase in descending pain modulatory system. J Signal Transduct 2011;2011:468061.
43. Estevez M, Estevez AO, Cowie RH, et al. The voltage-gated calcium channel UNC-2 is involved in stress-mediated regulation of tryptophan hydroxylase. J Neurochem 2004;88:102–113.

Received August 3, 2016. Accepted January 5, 2017.

Correspondence
Address correspondence to: Zhiyuan Gong, PhD, Department of Biological Sciences, National University of Singapore, Singapore 117543. e-mail: dbsgzy@nus.edu.sg; fax: (65)-67792486.

Acknowledgment
Chuan Yan, Qiqi Yang, and Zhiyuan Gong conceived and designed the experiments; Qiqi Yang and Chuan Yan performed the experiments; Qiqi Yang, Chuan Yan, Chunyue Yin, and Zhiyuan Gong analyzed the data; Chuan Yan, Qiqi Yang, and Zhiyuan Gong wrote the paper; and Chunyue Yin provided material.

Conflicts of interest
The authors disclose no conflicts.

Funding
Supported by research grants from the National Medical Research Council and the Ministry of Education of Singapore. The sponsors had no role in the study design, or the collection, analysis, or interpretation of data.